ELSEVIER

International Journal of Mass Spectrometry 214 (2002) 1–21

International Journal of Mass Spectrometry

www.elsevier.com/locate/ijms

Review

Gas-phase chemistry of actinide ions: probing the distinctive character of the 5f elements

John K. Gibson

Chemical Sciences Division, Oak Ridge National Laboratory, Bldg. 5505, P.O. Box 2008, Oak Ridge, TN 37831-6375, USA

Received 20 August 2001; accepted 30 October 2001

Abstract

Recent years have witnessed an increased level of activity in the study of gas-phase chemistry of bare and oxo-ligated actinide ions. The intent of this report is to summarize some key accomplishments in gas-phase actinide ion chemistry. Early work on thorium and uranium is described along with an account of recent results for the more radioactive synthetic actinides. Reactions of bare and oxo-ligated actinide ions with hydrocarbons have been a central focus of study and reveal important insights into actinide chemistry. Also briefly summarized are a few representative reactions with other types of substrates. Some results for the homologous lanthanide elements are included for comparison. Other types of reactions are also considered with an emphasis on the unique behavior of the actinides. Future prospects in the field of gas-phase actinide ion chemistry are discussed. (Int J Mass Spectrom 214 (2002) 1–21) © 2002 Elsevier Science B.V. All rights reserved.

Keywords: Actinides; 5f Elements; Lanthanides; Metal ion chemistry

1. Background

Investigations of gas-phase chemistry of metal ions have been carried out for more than three decades. Early studies included association processes, particularly hydration of alkali metal ions [1,2]. Acid–base reactions of Li^+ with organics were among the first gas-phase metal ion chemistry which involved bond cleavage [3]. A seminal development in gas-phase metal ion chemistry was the demonstration in the late 1970s by Ridge and co-workers that transition metal ions can activate C–H and C–C bonds [4,5]. In the past two decades a substantial effort has been dedicated to hydrocarbon activation, particularly by first row transition metal ions, Sc^+ through Zn^+. A primary focus has been on understanding the effects of the electronic configurations and energetics at the metal center on activation processes [6–12]. Although many aspects of gas-phase metal ion chemistry bear relevance to condensed phase processes [13], a central rationale for the studies described here is to enhance fundamental understanding of transition metal chemistry, particularly that of the f-block "inner" transition metals.

Gas-phase metal ion chemistry studies of the f-block inner transition elements have recently received increasing attention due to their distinctive electronic structures and chemical properties. The lanthanide elements, La through Lu, generally exhibit similar condensed phase chemistry, with the trivalent oxidation state prevalent under most conditions.

E-mail: gibsonjk@ornl.gov

1387-3806/02/$20.00
PII S1387-3806(01)00559-0

However, divalent or tetravalent chemistry is rather common for a few members of the series: e.g., Eu(II) and Ce(IV) [14]. The generally consistent condensed phase chemistry among the lanthanides reflects the sequential filling of the seven 4f orbitals which are spatially contracted and not chemically engaged under moderate physicochemical conditions. In distinct contrast to the rather uniform condensed phase behavior across the lanthanide series, it has been shown that the monopositive lanthanide ions, Ln^+, exhibit large variations in gas-phase chemistry. The discrepancies between gas-phase lanthanide ion chemistry and condensed phase lanthanide chemistry illustrate the important effects of inter-molecular interactions in the condensed phase. An early study of the appearance potentials of $LnCp^+$ from $LnCp_3$ (Ln = Nd, Sm, Yb; Cp = cyclopentadienyl) [15] revealed a correlation between organometallic bond energies and the electronic structure of the lanthanide. Several subsequent studies have pursued the role of Ln^+ electronic structures in gas-phase reactions with hydrocarbons [16–27]. Scandium, though not an f-block element, is in group 3 and lanthanide chemistry is generally similar to that of Sc. Tolbert and Beauchamp [28] concluded that gas-phase hydrocarbon activation by Sc^+ proceeds by an insertion mechanism which employs the two remaining valence electrons at the metal ion center to form a C–Sc^+–H (for dehydrogenation) or C–Sc^+–C (for cracking) intermediate. Schilling and Beauchamp [17] had postulated that two non-4f electrons were needed at a Ln^+ metal center to enable hydrocarbon activation by a mechanism similar to that for Sc^+. This proposal, supported by results of Yin et al. [21], was confirmed by a systematic study with all Ln^+ (except Pm^+) by Cornehl et al. [23]; the results of other studies are consistent with this hydrocarbon activation model. The necessity for two non-4f valence electrons for effective insertion reflects that the valence 4f orbitals, unlike the outer d-orbitals of the d-block transition elements, are spatially localized relative to the outer valence electrons and do not participate in chemical bonding [29]; this leads to the usage of "quasi-valence" to characterize the 4f electrons (orbitals) of the lanthanides. A result of the inert character of the quasi-valence 4f electrons is that the efficiency of the Ln^+ ions at gas-phase activation of hydrocarbons correlates with the promotion energy from the ground state electronic configuration to the lowest-lying $[Xe]4f^{n-2}5d^16s^1$ configuration, denoted $\Delta E[Ln^+]$. These promotion energies range from 0 for Gd^+ ($4f^75d^16s^1$ ground state) to 3.8 eV for Eu^+ ($4f^76s^1 \rightarrow 4f^65d^16s^1$) [30]. Accordingly, Gd^+ rather efficiently activates 1-butene whereas Eu^+ is nearly inert towards this reagent; the reaction rates of the other Ln^+ are in accord with their intermediate ΔE values [30]. An important finding of the Ln^+ studies [23] was the significantly reduced reactivity of Lu^+. The ground state of Lu^+ is $4f^{14}6s^2$, indicating that excitation to the $4f^{14}5d^16s^1$ configuration, $\Delta E[Lu^+\{4f^{14}6s^2 \rightarrow 4f^{14}5d^16s^1\}] = 141\,kJ\,mol^{-1}$, is necessary for insertion and that the electrons in the filled $6s^2$ sub-shell are inert.

1.1. The actinides

The actinides are the 5f homologs of the lanthanides, with the 5f valence orbitals being filled between Ac and Lr. The physical and chemical properties of the two series of f-block transition elements are substantially different. Notably, Cotton and Wilkinson [29] identify the lanthanides as La through Lu but refer to "actinium, thorium, protactinium and the actinide elements", implying that the actinide series begins at U. However, we consider here the actinides to comprise the entire series, Ac through Lr. Whereas the lanthanides are all rather similar in their condensed phase chemistries, substantial differences in this chemistry are found between the homologous actinide and lanthanide elements, as well as between the members of the actinide series. The early actinides (through Pu) are particularly differentiated from the homologous early lanthanides in two major regards. Firstly, the actinides exhibit a variety of oxidation states, from a maximum state for Ac of +3 up to +7, for Np. Comparing two homologs between the series, Nd^{3+} is the highest oxidation state under moderate physical/chemical conditions whereas U(VI) is easily

obtained, as in UF_6 and the ubiquitous uranyl ion, UO_2^{2+} [31]. Higher oxidation states of Nd (e.g., +4) and other lanthanides can be obtained under extreme conditions, such as upon exposure to potent oxidants and as high temperature vapor species. A second major difference between the actinides and lanthanides is that the 5f electrons (and perhaps also vacant 5f orbitals) of the early actinides can participate directly in bonding, in sharp contrast to the localized nature of the 4f electrons of all of the lanthanides. The extremely complex structural and physical properties of Pu metal are directly attributable to involvement of the low-symmetry 5f orbitals in metallic (covalent) bonding [32]. Beyond Pu, the 5f orbitals are increasingly localized and generally do not participate in bonding. However, when transplutonium actinide metals are subjected to very high pressures non-bonding 5f electrons may become bonding due to decreased interatomic distances. Furthermore, stabilization of the 5f electrons for the heavy actinides results in a limitation of readily accessible oxidation states to II, III and/or IV. A particularly significant contrast between the two f-element series is that in contrast to the late lanthanides, where the trivalent oxidation state is common, divalence is dominant for the actinides beyond Cf. A primary motivation for studying gas-phase actinide ion chemistry is to better understand the unique character of the electronic structures and energetics of the actinides, and particularly both the direct and indirect roles of the 5f electrons. Most of the distinctive chemistry of the actinides can be traced either directly or indirectly to the changing character of the 5f electrons. The electronic structure and energetics of the actinides are more affected by relativistic effects than lighter elements due to the high nuclear charge. Relativistic effects are central in understanding the unique chemical behavior of the actinides and specifically the energetics of electronic configurations. Essentially, the 5f electrons are relatively high in energy and spatially extended for the early actinides, resulting in high oxidation states and/or direct participation of the 5f electrons in bonding. As the nuclear charge increases, the 5f electrons become increasingly stabilized and spatially contracted (localized) relative to the valence 6d and 7s electrons.

Fig. 1 summarizes key information about the electronic structures and energetics of the actinide monopositive ions, An^+. The promotion energies in Fig. 1 correspond to the transition from the lowest *J*-level of the ground state term to the lowest *J*-level of the excited state term. This is in contrast to averaging over *J*-levels for a given term as is often done in similar considerations of d-block transition metal ion chemistry. For the d-block transition metals, and particularly the 3d series, the term splitting is relatively small compared with the actinides. For example, the $J = 3/2$, 5/2, 7/2 and 9/2 levels of the ^{4}F [Ar]$3d^2 4s$ ground state configuration of Ti^+ range in energy from 0 to only 393 cm^{-1} (4.8 kJ mol^{-1}). In contrast, the $J = 9/2$, 11/2, 13/2, 15/2 levels of the ^{4}I [Rn]$5f^3 7s^2$ ground state configuration of U^+ range in energy from 0 to 11,708 cm^{-1} (142 kJ mol^{-1}). As discussed later, it is apparent that the spectroscopically-derived lowest energy levels for the ground and excited states of the An^+ correlate well with the observed gas-phase ion chemistry, and evidently it is not appropriate to average over the *J*-values of the configuration terms. This does not necessarily imply Russell–Saunders coupling rather than the *jj*-coupling which is expected for these high atomic number atoms. Instead, the interpretation is that the free ion population is dominated by the specified lowest-lying configuration with a high degree of spin–orbit coupling. The lowest energy level of the configuration is conventionally identified according to ill-defined values of *S* and *L*. Similarly, the values of *S* and *L* for the excited state configuration may not be particularly meaningful, but the energy of the lowest lying member of the spectroscopic manifold is valid for predicting the promotion energy, ΔE. In those cases, where a ground or excited state configuration exhibits closely-spaced levels it may be more appropriate to employ some sort of averaging among these contributing levels but such a relatively minor modification would not appreciably alter the interpretation of the results in the context of electronic excitation.

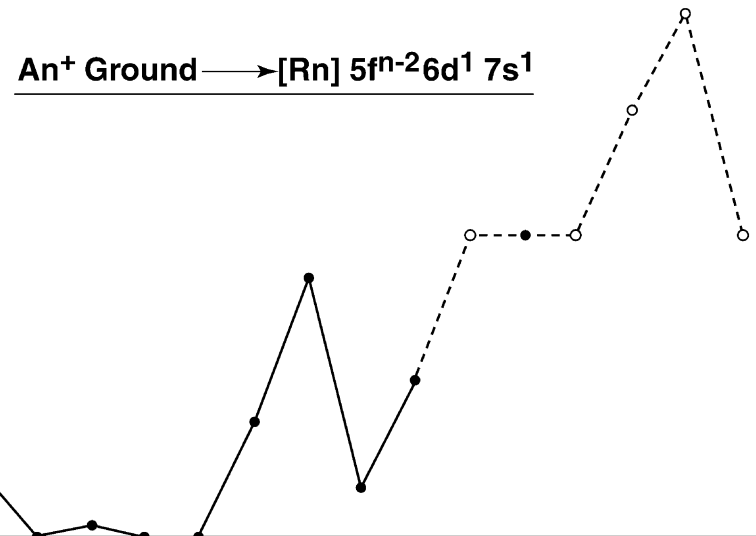

	Ac	Th	Pa	U	Np	Pu	Am	Cm	Bk	Cf	Es	Fm	Md	No	Lr
ΔE (eV)	0.6	0.0	0.1	0.0	0.0	1.1	2.5	0.5	1.5	*2.9*	2.9	*2.9*	*4.1*	*5.0*	*2.9*
Ground State 5f	0	0	2	3	4	6	7	7	9	10	11	12	13	14	14
Ground State 6d	0	2	0	0	1	0	0	0	0	0	0	0	0	0	0
Ground State 7s	2	1	2	2	1	1	1	2	1	1	1	1	1	1	2
	d-block		5f-bonding				5f-localized								

Fig. 1. Actinide monopositive ion electronic structures and energetics. The ground state configuration is given for each An^+ as the number of 5f, 6d and 7s electrons outside of the filled radon core. The energies, ΔE, are for promotion from the ground state to the "divalent" $[Rn]5f^{n-2}6d^17s^1$ configurations (eV); the values in italics are estimates (the value for Cf^+ may not correspond to the lowest level of the configuration). The promotion energies are from Blaise and Wyart [33] except for the estimates for Md^+, No^+ and Lr^+ from Brewer [34]. The magnitudes of these promotion energies are represented graphically by the connected circles; unfilled circles and dashed connecting lines correspond to estimates. For Th^+, the $6d^27s^1$ ground state should be the most reactive; $\Delta E[Th^+]$ is thus given as 0 rather than the value of 0.6 eV for excitation to the $5f^16d^17s^1$ configuration. The $5f^{n-2}6d^2$ configuration does not lie below the $5f^{n-2}6d^17s^1$ configuration for any An^+. The postulated role of the 5f electrons in the elemental metals is indicated at the bottom of the figure.

Also indicated in Fig. 1 is a rough division of the actinide elements according to their metallic bonding character under normal (STP) conditions: d-like (Ac, Th); f-bonding (Pa–Pu); or f-localized (Am–Lr). The ground state configurations of Ac^+ and Th^+ have no 5f electrons, and gas-phase chemical behavior characteristic of the corresponding d-block metal ions would be expected: Ac^+ should behave approximately similarly to $La^+/Y^+/Sc^+$; and Th^+ similarly to $Hf^+/Zr^+/Ti^+$. It should be noted that significant variations are evident in the chemistries of d-block transition elements within a given group. Beyond Th^+ the seven 5f orbitals are filled in the fairly regular sequence indicated in Fig. 1. The particular stability of the $5f^7$ half-filled shell results in a $5f^77s^2$ (rather than $5f^87s^1$) ground state for Cm^+. Based on the demonstrated correlation between Ln^+-induced hydrocarbon activation and the ground to "divalent" promotion energies, $\Delta E[Ln^+]$, it might be expected that the analogous $\Delta E[An^+]$ given in Fig. 1 would have a comparable effect in actinide ion chemistry. However, direct participation of the actinide 5f electrons in bonding might allow certain reactions to proceed without promotion to an outer 6d orbital, resulting in greater than predicted reactivities, especially for the lighter actinides; this issue is fundamental to gas-phase actinide

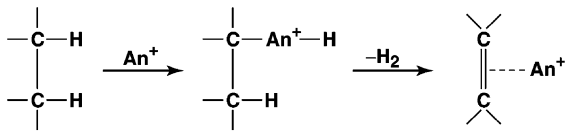

Scheme 1.

ion chemistry. As for the lanthanides, it is presumed that hydrocarbon activation–dehydrogenation and cracking-by An^+ generally proceeds according to an insertion mechanism, as shown for dehydrogenation in Scheme 1, where the HC–CH moiety represents an activation site of a generic hydrocarbon (alkane, alkene or alkyne). Accordingly, reactions of An^+ with hydrocarbons are expected to be particularly informative regarding the role of electronic structures and energetics in gas-phase actinide ion chemistry, actinide organometallic chemistry, and actinide chemistry in general.

As Cornehl et al. noted in the context of their lanthanide results [23], secondary effects besides $\Delta E[Ln^+]$ certainly influence reaction efficiencies but this fundamental parameter is very useful in assessing the gas-phase organometallic reactivities of Ln^+. Also, interpretation of the results in terms of the elementary mechanistic model in Scheme 1 ignores the details of the insertion process which proceeds along a potential energy surface and may involve significant kinetic barriers, including evident formal loss of spin-conservation. A simplistic explanation for the phenomenological observation that the formal spin may vary during a reaction without appreciably affecting the rate is that weak spin–orbit coupling (Russell–Saunders coupling) does not apply to the heavy metal ions being studied. Instead, strong spin–orbit coupling (*jj*-coupling) better describes the electronic states and the requirement for spin-conservation is thereby relaxed. To the extent that some requirement for spin-conservation may be relevant to lanthanide and actinide ion chemistry, the concept of *two-state reactivity* can be invoked to explain the occurrence of otherwise apparently forbidden reaction pathways [35]; essentially it is proposed that reactions can proceed along pathways which involve a rate-determining step of spin inversion, if required.

2. Reactions of Th^+ and U^+ with hydrocarbons

Early studies of actinide ion chemistry were limited to the two abundant long-lived actinides, thorium and uranium. In 1977, Armentrout et al. reported on a study of endothermic reactions of U^+ with CD_4 (and other molecules) using a guided ion beam apparatus [36,37]. Their results for the $U^+ + CD_4$ reaction are reproduced in Fig. 2. From the onset collisional energy for the specified reaction, a U^+–D bond dissociation energy of 3.0 eV and a proton affinity of the uranium atom of 10.3 eV were derived [37]. This very large proton affinity (vs. 8.4 eV for Li) was attributed to the combination of a small ionization energy of uranium and the formation of a strong covalent bond between uranium and hydrogen. Although these initial studies provided fundamental thermodynamic information, neither the reaction mechanism nor the potential role of the 5f electrons was directly assessed.

Within the last decade a handful of studies have been carried out for reactions of Th^+ and U^+ with alkanes and alkenes by Fourier transform-ion cyclotron resonance mass spectrometry (FT-ICR–MS) [38–41]. In the first description of such FT-ICR–MS experiments [38] it was stated that U^+ activates 1,3,5-tri-*t*-butylbenzene, but the report was preliminary and quantitative results were not given.

Heinemann et al. [39] carried out the first comprehensive and quantitative FT-ICR–MS study of a series of reactions of U^+ with several hydrocarbons. They found substantial reactivity for U^+, particularly compared with its 4f congener, Nd^+. This can be understood in the context of an insertion mechanism (Scheme 1) and the substantial difference in promotion energies to achieve a "divalent" state: $\Delta E[U^+\{5f^37s^2\} \rightarrow \{5f^36d^17s^1\}] = 0.03\,eV$ vs. $\Delta E[Nd^+\{4f^46s^1\} \rightarrow \{4f^35d^16s^1\}] = 1.4\,eV$. It is feasible that the 5f electrons of U^+, unlike the 4f electrons of Nd^+, can participate in bond activation but the results for U^+ do not directly address

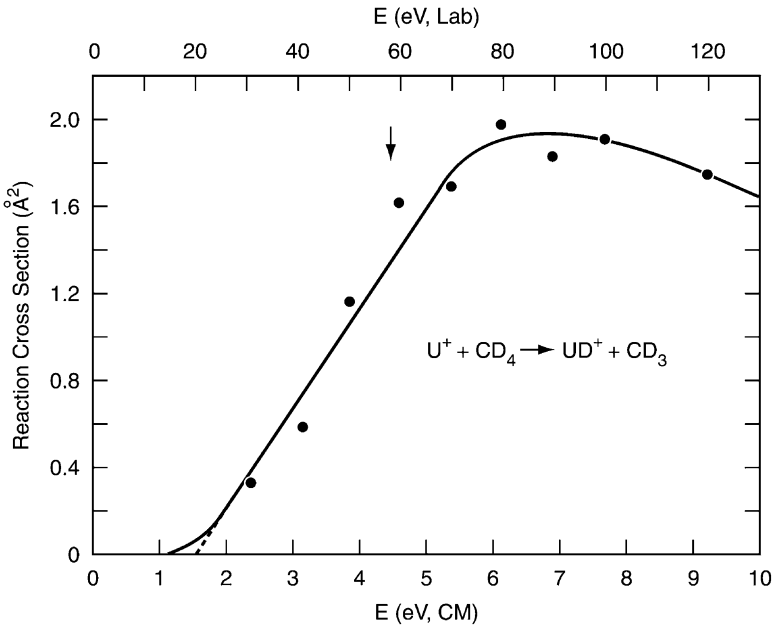

Fig. 2. Results from an early guided ion beam study of the reaction of U^+ with CD_4. Reproduced with permission from "endothermic reactions of uranium ions with N_2, D_2, and CD_4" [37]. Copyright 1977 Am. Inst. Phys.

this issue because of the extremely small energy (0.03 eV ≈ 300 K) for excitation of a 7s electron to a 6d orbital. It was also demonstrated that U^+ catalyzes trimerization of ethylene to benzene in a three-step process according to the overall Reaction (1):

$$U^+ + 3C_2H_4 \rightarrow U^+ \cdot C_6H_6 + 3H_2 \quad (1)$$

A similar study of reactions of Ln^+ with hydrocarbons was carried out in the same laboratory [23] and it is instructive to compare the reaction rates reported for representative lanthanide ions with those for U^+. With propane, for example, the activation efficiencies, k/k_L, were 0.45 for La^+, 0.15 for Ce^+, 0.05 for Gd^+, and 0.02 for U^+; in all cases the H_2-loss and $2H_2$-loss branching ratios were roughly comparable. This comparison would seem to suggest that the increasing density of 4f electrons between La^+ (zero 4f electrons) and Gd^+ (seven 4f electrons) and, perhaps to a greater extent, the presence of three 5f electrons for U^+ may actually inhibit insertion of a metal ion into an alkane C–H bond, perhaps by a repulsive interaction. All four metal ions activated propene and cyclopropane with similarly high efficiencies. However, for Gd^+ and U^+, H_2-loss was the sole channel whereas for La^+ and Ce^+, H_2-loss and C_2H_4-loss (giving $LnCH_2^+$) were of roughly equal importance. Although U^+ chemistry is evidently somewhat disparate from that of La^+ and Ce^+, the approximate similarity between U^+ and Gd^+ argues against a particularly distinctive role for the 5f electrons of the uranium ion, at least for the studied reactions.

Marçalo et al. [40] carried out the first study of reactions of Th^+ with hydrocarbons and found a very high reactivity. Even methane was activated to produce $ThCH_2^+$, presumably in an exothermic process. This contrasts with the behavior of U^+ [39] which failed to react with either methane or ethane. This and other comparisons with the earlier work with U^+ [39] led to the conclusion that Th^+ is more reactive than both U^+ and the most reactive Ln^+ ions, including its 4f congener, Ce^+. In essence, Th^+ does indeed appear to behave as a highly reactive d-block transition metal ion, in accord with its "trivalent" ground state configuration, $6d^2 7s^1$.

Table 1
Efficiencies of reactions of actinide ions with arenes[a]

	Reaction efficiency[b]						
	Th^+	U^+	ThO^+	UO^+	UO_2^+	Th^{2+}	U^{2+}
Benzene	0.26	0.11	0.05	0.02	0.02	0.66	0.44
Benzene-d_6	0.51	0.27		Not reported		0.59	0.46
Naphthalene	0.78	0.51	0.40	0.16	0.42	0.90	1.36
Toluene	0.38	0.30	0.13	0.03	0.10	0.51	0.77
Mesitylene	0.94	0.46	0.37	0.19	0.45	0.80	1.39
Hexamethylbenzene	1.01	0.69	1.58	0.48	1.41	0.96	1.38
1,3,5-Tri-*t*-butylbenzene	2.67	1.15	2.02	0.82	1.63	1.02	0.78

[a] Adapted with permission from "gas-phase actinide ion chemistry: FT-ICR–MS study of the reactions of thorium and uranium metal and oxide ions with arenes" [41].

[b] The overall reaction efficiencies are k/k_L which is the reaction efficiency as a fraction of the Langevin collisional rate, k_L. For toluene, k_{ADO}, the average dipole orientation theory collisional rate is used in place of k_L [41]. The dominant reaction pathways were H_2-elimination or cracking for An^+, adduct formation for AnO_n^+, and charge transfer for An^{2+}; less dominant channels are noted in the text.

Marçalo et al. [41] subsequently reported on a comparative FT-ICR–MS study of reactions of bare and oxo-ligated thorium and uranium ions with several arenes. Their results are summarized in Table 1 as net reaction efficiencies; the oxide ion results included in Table 1 are discussed in a later section. The primary reaction channels for Th^+ and U^+ were loss of dihydrogen and/or small hydrocarbons: C–H and C–C activation was dominant. The values for Th^+ and U^+ in Table 1 indicate rather high reactivities and confirm a somewhat greater reactivity of Th^+ compared with U^+. The k/k_{ADO} value of 2.67 for the reaction of Th^+ with 1,3,5-tri-*t*-butylbenzene suggests significant uncertainties in the absolute efficiency values; however the comparisons between Th^+ and U^+ for a given reactant molecule should be substantially more reliable. The greater reactivity of Th^+ may relate to the availability of a 7s and two 6d electrons in its ground state. Another apparent difference was the greater propensity for Th^+ to induce C–C activation compared with U^+. As with U^+, the high reactivity of Th^+ does not illuminate the role of the 5f electrons because both Th^+ and U^+ have at least two non-5f electrons in their ground state (Th^+) or very low-lying (U^+) configurations. Yin et al. [21] had studied reactions of Ln^+ with 1,3,5-tri-*t*-butylbenzene under similar conditions. The reported reaction efficiencies for the Ln^+ were in the range of 0.7–1.4. For Sm^+, Eu^+, Tm^+ and Yb^+, adduct formation was the only reaction channel whereas bond activation was dominant for all other Ln^+. To a first approximation, the bond activation reactivity of U^+ with 1,3,5-tri-*t*-butylbenzene appears roughly comparable to those of the reactive Ln^+, further indication of no unique role for the 5f electrons or vacant 5f orbitals.

A particularly intriguing result from the work of Marçalo et al. [41] was for reactions of the doubly-charged ions, Th^{2+} and U^{2+}. In Table 1 it is seen that these An^{2+} reacted rather efficiently with each arene. In contrast to the monopositive ions, no consistent difference between the overall reaction efficiencies of Th^{2+} and U^{2+} was evident. For both Th^{2+} and U^{2+}, charge transfer typically accounted for ~3/4 of the overall "reaction efficiencies" given in Table 1. The remaining ~1/4 of reaction products resulted from arene bond activation, resulting primarily in loss of one or more hydrogen molecules and/or stable hydrocarbon fragments; transfer of H^- or CH_3^- to An^{2+} also appeared as minor channels. Because the reaction mechanisms may be entirely different for the singly and doubly charged ions, the absolute efficiencies should not be directly compared according to the same model; if the same mechanism were operative, a greater activation efficiency would generally be anticipated for M^{2+} ions. As Marçalo et al. pointed out [41], the substantial reactivities of

Th^{2+} and U^{2+}, and the latter in particular, may be suggestive of direct involvement of the 5f electrons in bonding during the activation process. The ground state of Th^{2+} is $Rn[5f^16d^1]$, with the $Rn[6d^2]$ configuration only 0.8 kJ mol^{-1} higher in energy; the ground state of U^{2+} is $Rn[5f^4]$, with the $Rn[5f^36d^1]$ configuration only 2.5 kJ mol^{-1} higher in energy. Promotion of a second 5f electron of U^{2+} to an outer valence orbital requires at least 230 kJ mol^{-1}. The very low energy for promotion of a single 5f electron to a 6d orbital for these light An^{2+} allows assessment of their behavior in the context of the presumably more reactive low-lying excited states. An alternative to the direct participation of 5f electrons in U^{2+} chemistry is that the greater charge on the metal center enables elimination processes by mechanisms other than the analog of the insertion mechanism shown in Scheme 1 where An^+ is replaced by An^{2+}. The very similar reactivities of Th^{2+} and U^{2+} would seem to support an alternative type of activation mechanism because a significant difference in bonding efficiencies would be predicted for the low-lying $6d^2$ configuration of Th^{2+} compared with the low-lying $5f^36d$ configuration of U^{2+}. The results for reactions of La^{2+} with alkanes carried out by Freiser and co-workers [19] are particularly instructive in interpreting the Th^{2+}/U^{2+} results. The La^{2+} ion has a similar electron affinity to Th^{2+} and U^{2+}: 11.1 eV for La^{2+} vs. 11.9 eV for both Th^{2+} and U^{2+}; most significantly, La^{2+} has only one valence electron outside of the closed xenon core, with a $[Xe]5d^1$ ground state [30]. It was found that La^{2+} induces loss of H_2 and hydrocarbon fragments from propane and butane, almost certainly via an ion–neutral interaction mechanism not involving direct insertion into a C–H or C–C bond [19] because of the dearth of available valence electrons at the metal center. A similar non-insertion mechanism may well be operative for Th^{2+} and/or U^{2+}, with the 5f electrons in a passive role. The absence of valence 7s electrons in the ground and low-lying configurations of Th^{2+} and U^{2+} may also be relevant to understanding their reactivities in comparison with the An^+ ions. The reactivities of these and other doubly-charged actinide and lanthanide ions certainly deserve further attention.

3. Reactions of other An^+ with hydrocarbons

The actinide ion chemistry studies discussed to this point have been limited to Th^+ and U^+ because of the inability to handle the more highly radioactive actinides in conventional laboratories and instruments. As already noted (Fig. 1), it is necessary to study several additional actinides to establish the role of electronic structure and energetics, particularly 5f effects. The intrinsically reactive ground state configurations of Th^+ and U^+ are such that the distinctive nature of the 5f elements is not directly illuminated in their chemistries. Accordingly, we have undertaken to study the gas-phase chemistry of additional actinide ions in the Transuranium Research Laboratory at Oak Ridge National Laboratory. Because of the need for rigorous containment of highly radioactive synthetic elements, most of which undergo alpha decay, it was necessary to design an apparatus which could be installed inside of an alpha-containment glovebox. This initial apparatus was accordingly relatively rudimentary and absolute reaction rates and cross-sections could not be determined, in contrast to the earlier FT-ICR–MS experiments with Th^+ and U^+. Instead, the primary goal was to systematically compare the bond activation efficiencies of the actinide ions across the series.

The experiment is shown schematically in Fig. 3. Both the apparatus and experimental methodologies have been described elsewhere [25,27,42] and only a brief description is included here. A pulsed XeCl excimer laser ($\lambda = 308$ nm) is focused onto a copper target containing a few atomic percent of one or more metal oxides. Ablated ions (and neutrals) traverse a $\sim$3 cm long reaction zone containing a reagent at an indeterminate pressure; appearance of bis-adducts suggested that the pressure was generally sufficient that a substantial fraction of the ablated ions encounter one or more reactant molecules. After a time delay following the laser pulse, t_d, of typically $\sim$40 μs the positive ions, both unreacted and products, are injected orthogonally into the flight tube of a reflectron time-of-flight mass spectrometer by application of a +200 V pulse to the repeller plate at the back of the

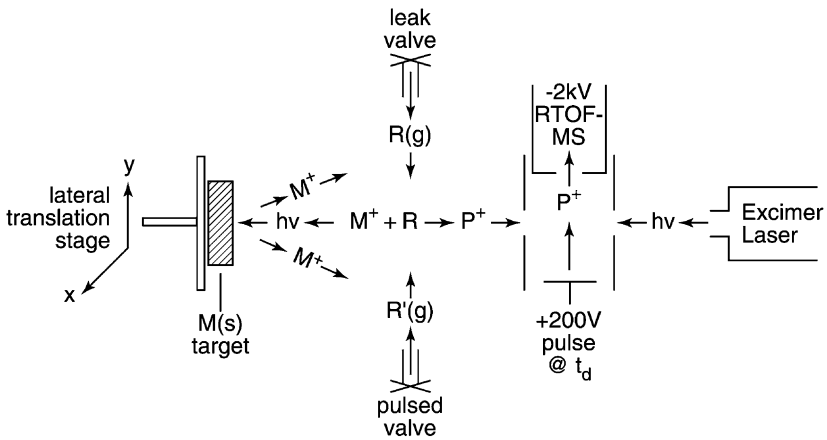

Fig. 3. Schematic of the LAPRD apparatus used at ORNL. Reproduced with permission from ref. [25]. Copyright 1996 Am. Chem. Soc.

ion source region. The mass spectrometer resolution is ∼1000, which provides unit mass discrimination for all of the studied ions. Because absolute reaction rates (cross-sections) are not obtained, generally two or more metal ions are studied simultaneously to allow for direct and quantitative comparison of relative reactivities and reaction branching ratios. The source region of the mass spectrometer is contained within a glovebox in an alpha laboratory and all sample handling is performed within this and other gloveboxes to prevent release of radioactive contamination. The technique is referred to as laser ablation with prompt reaction and detection (LAPRD) and is similar to the *laser ablation-molecular beam* method described by Sato and co-workers [43].

Laser-ablated ions are often in excited electronic states and the LAPRD approach employs reactions of nascent ablated ions. Accordingly, it might be expected that excited state metal ion chemistry would be important. A systematic study of lanthanide ion chemistry was carried out prior to proceeding to the actinides to explore this possibility [25]. The results for Ln^+ were in good agreement with those from an FT-ICR–MS study [23] where ground state Ln^+ behavior had been confirmed. All subsequent LAPRD studies have revealed no evidence for excited state chemistry. Although we have proposed explanations for the absence of excited state metal ion chemistry in LAPRD, it essentially remains a phenomenological observation.

The initial focus was on reactions of actinide ions with hydrocarbons. Results have been reported for Th^+, U^+ [27]; Np^+, Pu^+ [42]; Am^+ [44]; Cm^+ [45]; Bk^+ [46], and Cf^+ [47]. We have also obtained preliminary results for Pa^+ [48], and Es^+ [49]. When practical, the least radioactive isotope available in sufficient quantities is employed for the LAPRD studies—for example, ^{242}Pu (half-life = 375,000 years) rather than ^{239}Pu (24,100 years); and ^{243}Am (7370 years) rather than ^{241}Am (433 years). The shortest-lived isotope successfully studied was ^{253}Es which has a half-life of 20 days; this target contained only ∼50 μg of ^{253}Es (and an equal amount of its ^{249}Bk daughter). More typically at least ∼1 mg of the actinide of interest was employed. It was not possible to detect Fm^+ ablated from a target containing only 1 ng of ^{255}Fm (half-life = 20 h) by the LAPRD technique [49]; this negative result reflects the relatively low sensitivity of the LAPRD technique compared with trapped ion mass spectrometries.

Representative LAPRD results for reactions of bare actinide ions with hydrocarbons are shown in Figs. 4 and 5. To obtain the time-of-flight mass spectrum in Fig. 4, a target containing $^{237}NpO_2$ and $^{243}AmO_2$ was ablated into cyclohexene [44]. The two dominant ions, Np^+ and Am^+, were ablated in roughly equal

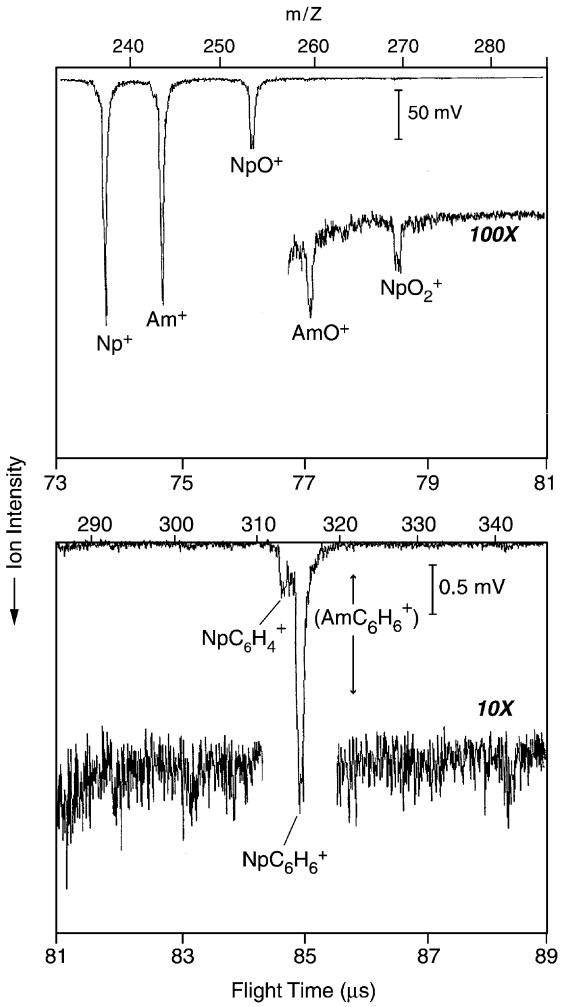

Fig. 4. LAPRD mass spectrum for the reactions of Np^+ and Am^+ with cyclohexene. The upper panel shows the mass region of reactant ions and the lower panel shows the mass region with product ions. Reproduced with permission from ref. [44]. Copyright 1998 Am. Chem. Soc.

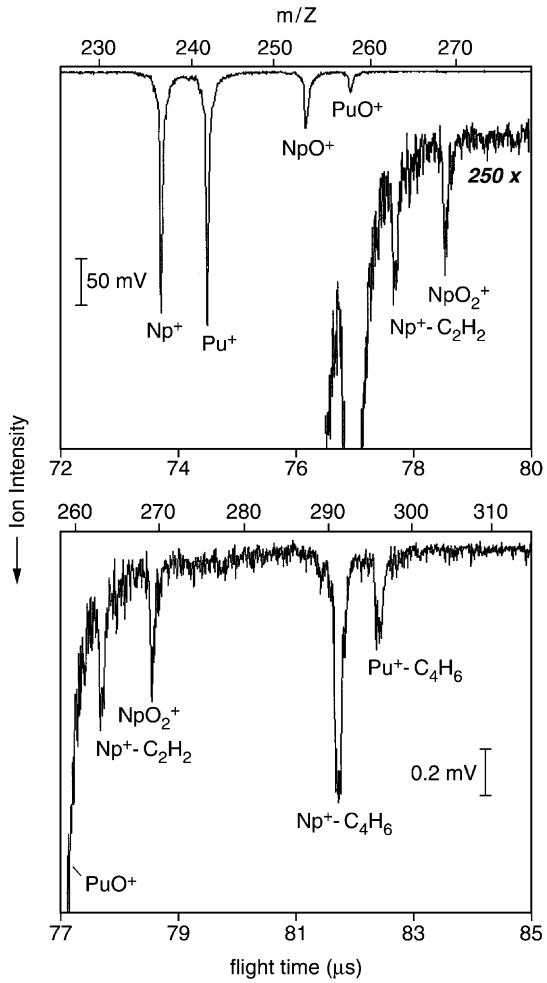

Fig. 5. LAPRD mass spectrum for the reactions of Np^+ and Pu^+ with 1-butene. The upper panel shows the mass region of reactant ions and the lower panel shows the mass region with product ions. Reproduced with permission from ref. [42]. Copyright 1998 Am. Chem. Soc.

amounts; the unreacted ions, evident in the top panels of the spectra, were usually in much greater abundance than the products. Products ions are identified in the bottom panel of Fig. 4; only neptunium products were detected but the location where the hypothetical americium product, $AmC_6H_6^+$, would have appeared is also indicated. The Np^+ mainly induced $2H_2$-loss to give $NpC_6H_6^+$, presumably a π-bonded Np^+–benzene organometallic complex. A minor reaction channel was $3H_2$-loss to give $NpC_6H_4^+$, presumably a Np^+–benzyne complex with stronger, σ-type organometallic bonding. In contrast, Am^+ was apparently inert under identical reaction conditions—the absence of any discernible americium products indicates a reaction cross-section with this substrate more than two orders of magnitude smaller for Am^+ compared with Np^+. By selecting more reactive reagents, such as cyclooctadiene, it was possible to observe reactions of

even relatively inert ions such as Am^+. However, Am^+ was consistently less reactive than Np^+ and other reactive An^+. In Fig. 5, are shown results for the simultaneous reaction of approximately equal amounts of $^{237}Np^+$ and $^{242}Pu^+$ with 1-butene [42]. The lower reactivity of Pu^+ compared with Np^+ is clearly evident from the relative yields of the dehydrogenation products, $AnC_4H_6^+$, presumably An^+–butadiene complexes. An even more dramatic demonstration of the greater reactivity of Np^+ was the appearance of the cracking product, $NpC_2H_2^+$ (Np^+–acetylene), with no evidence for corresponding Pu^+-induced C–C activation. A $PuC_2H_2^+$ product would have appeared at one mass unit below NpO_2^+ (i.e., at *m*/*z* 268) and the mass resolution is sufficient that this peak would have been evident.

Because appreciable amounts of certain AnO^+ were ablated along with bare An^+ in the LAPRD experiments, the possibility of reaction channels attributed to An^+ actually resulting from reactions of AnO^+ must be considered. For several lanthanides, as well as thorium and uranium, substantial amounts of MO^+ were ablated in LAPRD experiments. The consistency of LAPRD results attributed to lanthanide, thorium and uranium bare metal ion chemistry with those from mass-selected FT-ICR–MS experiments indicates that the metal oxide ion chemistry did not confuse interpretation of LAPRD results. A particular process which was emphasized as indicative of intrinsic An^+ chemistry was C–H activation which results in dehydrogenation. In support of the experimental evidence for a minimal contribution due to An^+–O bond cleavages, thermochemical considerations indicate that such processes should be insignificant under LAPRD conditions. Specifically, dehydration by AnO^+ would result in products indistinguishable from those due to dehydrogenation by bare An^+ but dehydration is thermodynamically unfavorable. Significant amounts of AnO^+ were ablated only when the An^+–O bond dissociation energy was greater than $\sim$600 kJ mol^{-1}; actinide oxide ions in substantial abundance were ThO^+, UO^+, NpO^+, PuO^+ and CmO^+. Among these five AnO^+ the smallest dissociation energy is $\sim$700 kJ mol^{-1}, for PuO^+. Because the enthalpy of formation of water is -242 kJ mol^{-1} (vs. 0 for H_2), M^+–O bond rupture to enable exothermic dehydration by oxide ions would require complex product ions which are stable by at least 460 kJ mol^{-1} more than required for exothermic dehydrogenation by bare metal ions. For example, dehydrogenation of 2-butene by Pu^+ to give $PuC_4H_6^+$, presumably a Pu^+–[1,3-butadiene] complex, requires a reasonable organometallic bond energy of 120 kJ mol^{-1} whereas dehydration by PuO^+ to yield the same complex would require an improbably large Pu^+–C_4H_6 bond energy of at least 580 kJ mol^{-1}. As with the monoxides, only dioxide ions with large OM^+–O bond energies were ablated in sufficient quantities to account for observed products by dehydration rather than dehydrogenation so that dehydration was thermodynamically unfavorable. A trapped ion mass spectrometry experiment with UO^+ and UO_2^+ carried out to substantiate the assignments of precursor reactant ions is described below. Based on experimental evidence and thermodynamic considerations it is concluded with confidence that M^+–O bond rupture was not significant in the LAPRD experiments and that the specific ion–molecule reactions could be reliably assigned.

We have carried out dozens of reactions with several hydrocarbons of varying susceptibilities to activation, mostly alkenes. For each actinide studied, direct comparison was made with at least one other actinide ion; in many cases lanthanides were also included for comparison. From the results for the eight thoroughly studied An^+, the following overall ordering of hydrocarbon activation cross-sections emerges:

$$Th^+ \approx U^+ \approx Np^+ > Cm^+ \gtrsim Pu^+ > Bk^+ > Am^+ \approx Cf^+$$

Preliminary results for Pa^+ [48] indicate a very high reactivity, roughly comparable to that of Th^+, while those for Es^+ [49] indicate nearly inert behavior, similar to Cf^+. The LAPRD studies of Pa^+ and Es^+ will be completed and reported in the near future.

Referring to Fig. 1 it is evident that the above order of reactivities is in accord with the magnitudes of the $\Delta E[An^+]$ for promotion from the ground state

to an excited state with two non-5f valence electrons. That the reactivity of Cm^+ is significantly lower than that of Np^+ confirms that the closed $7s^2$ subshell is inert towards insertion and that excitation to the $6d^17s^1$ configuration is requisite. In accord with their "divalent" or "trivalent" (for Th^+) ground state or very low-lying electronic configurations, Th^+, U^+ and Np^+ are the most reactive An^+ studied. The LAPRD results for Th^+ and U^+ were in accord with those from FT-ICR–MS although the somewhat greater reactivity of Th^+ was not as clearly manifested in the semi-quantitative LAPRD method. In sharp contrast, Am^+ and Cf^+ were nearly inert with all reagents, in accord with their large $\Delta E[An^+]$. The three other An^+, Cm^+, Pu^+ and Bk^+, exhibited varying degrees of intermediate reactivity in accord with their respective $\Delta E[An^+]$ given in Fig. 1.

The correlation of the LAPRD results with excitation energies demonstrates that the insertion mechanism applicable to the lanthanides (Scheme 1) also applies to the monopositive actinide ions and that the 5f electrons of the actinide ions *beyond* Np^+ do not participate significantly in hydrocarbon activation by an insertion mechanism so that two non-5f valence electrons are required at the metal center to form the two covalent bonds in the activated intermediate. The agreement between the comparative An^+ reactivities confirms that the spectroscopically derived $\Delta E[An^+]$ are at least qualitatively reliable and can be used to predict actinide chemistry. In this regard, the transneptunium actinides behave in a similar fashion to the lanthanides. Because Th^+, U^+ and Np^+ each have a ground or very low-lying configuration with at least two unpaired non-5f valence electrons, their high reactivities do not illuminate the role of the 5f electrons for the light actinides. This is a particularly significant drawback to examining hydrocarbon activation by bare actinide monopositive ions because it is in this early region of the series where the 5f orbitals are the most spatially and energetically accessible and thus most likely to participate in organometallic bonding.

4. Reactions of actinide oxide ions with hydrocarbons

The general interest in gas-phase chemistry of oxo-ligated metal ions has been discussed elsewhere [50,51]. A primary motivation is to better understand condensed phase processes where neutral and charged metal oxide species are often of central importance. Also, the effects of perturbation of the electronic structure at the metal center can illuminate fundamental aspects of metal ion–molecule chemistry. For those metal oxides with weak M^+–O bonds (which does not apply to ablated AnO^+), oxidation can be a primary reaction pathway. The activation of hydrocarbons by actinide oxides is of special interest in the present context of understanding the electronic effects of the actinides vis-a-vis their intrinsic chemistry, and particularly the role of the 5f electrons in AnO_n^+ chemistry. The two essential processes by which one might expect non-oxidative activation by an AnO^+ ion to induce H_2-loss are illustrated in Schemes 2 and 3 where attack on a saturated portion of a generic hydrocarbon is simplistically represented for direct insertion (Scheme 2) and a multi-centered interaction (Scheme 3). Scheme 2 is the analogy of Scheme 1 for activation by a bare actinide ion, whereby the oxo-ligated metal center inserts into a C–H bond. Scheme 3 represents a very generalized electrostatic interaction between the oxide ion and the hydrocarbon

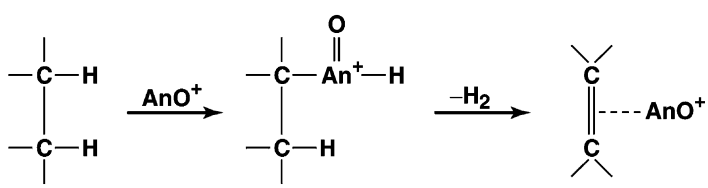

Scheme 2.

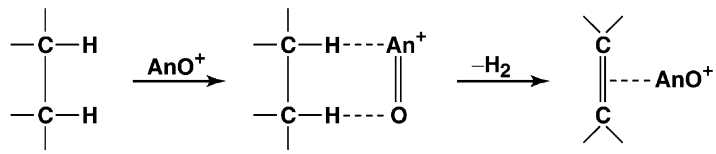

Scheme 3.

which results in activation and ultimate H_2-loss. It is emphasized that the elementary mechanisms represented in Schemes 2 and 3 are extreme simplified cases and that more complex intermediate activation processes are probable. In particular, the multicentered activation mechanism shown in Scheme 3 is arbitrary in suggesting simple activation of adjacent H-atoms via an electrostatic interaction. It is noted that similar generic mechanisms can be postulated for C–C activation by metal oxide ions.

Another feasible mechanism which can not be excluded by appears less probable is the direct insertion of an entire actinide oxide ion into a C–C bond to form an intermediate of the general form: $–C–An^+–O–C–$.

Cornehl et al. have examined reactions of lanthanide oxide cations with butadiene and isoprene [52]. They discovered a rather sharp increase in reactivity when the electron affinity of the LnO^+ was greater than some threshold value (i.e., with increasing ionization energy of neutral LnO). Also, the alkene with the lower ionization energy and greater nucleophilicity, isoprene, exhibited a reactivity onset for LnO^+ with smaller electron affinities. Their essential conclusion was that activation was proceeding by electrophilic attack on the diene. A metallaoxacycle was proposed as an intermediate; in essence, the LnO^+ formed a bridge between the two terminal carbons to form an activated complex susceptible to C–H and C–C bond cleavage. In a very general sense, the Scheme 3-type mechanism was operative. The absence of simple insertion (Scheme 2) was anticipated based on the absence of chemically active non-4f valence electrons at the metal center in Ln^+=O [52]. In a study of selected dioxide ions, Cornehl et al. [53] found that CeO_2^+ and ThO_2^+ efficiently oxidize alkenes to produce MO^+, and/or abstract an H-atom to produce $O{=}M^+–OH$ (M = Ce, Th). This is in accord with the difficulty to oxidize Ce and Th above the tetravalent state, and the correspondingly low values for the bond dissociation energies of the dioxide ions in which the metal center is *formally* pentavalent: $BDE[OCe^+–O] \approx 370\,kJ\,mol^{-1}$; $BDE[OTh^+–O] = 460\,kJ\,mol^{-1}$. In contrast, UO_2^+ is essentially inert, this in accord with the stability of the U(V) oxidation state and the resulting large value of $BDE[OU^+–O] = 740\,kJ\,mol^{-1}$, which is nearly as large as $BDE[U^+–O] = 770\,kJ\,mol^{-1}$ [54]. Reactions of the monoxide ions, MO^+ (M = Ce, Nd, Th, U) were also examined [53]. The authors make a convincing argument that CeO^+ (inert) can be considered as a 4f-block oxide cation and ThO^+ (reactive) as a d-block oxide cation, exhibiting similar behavior to ZrO^+. The inert character of NdO^+ is traced to the localized character of the 4f electrons at the trivalent metal center, and the somewhat greater reactivity of UO^+ to the involvement of the 5f electrons—this last interpretation is particularly significant.

In the study of Marçalo et al. [41], the reactivities of oxo-ligated as well as bare thorium and uranium ions were examined; the overall reaction rates for the three studied oxide ions are included in Table 1. For most of the reagents, and all with UO_2^+, adduct formation was the dominant reaction channel. The inert character of UO_2^+ vis-a-vis bond activation and oxidation accords with other results and the rationale presented. For ThO^+ and UO^+ reacting with hexamethylbenzene, H_2-elimination was an important channel, and with 1,3,5-tri-*t*-butylbenzene, CH_4-loss was the dominant channel. In accord with the results of Cornehl et al. [53], ThO^+ was found to be roughly three times as reactive as UO^+.

As is evident in Figs. 4 and 5, substantial amounts of the particularly stable actinide oxide ions were

ablated from the LAPRD metal oxide-in-copper targets. In those cases where adequate amounts of these ions were available, their chemistries could be evaluated by the LAPRD approach. Although no oxide ion reactions were apparent from the results in Figs. 4 and 5, such reactions were evident with other oxide ions and/or reagents. Results for the reactions of naked and oxo-ligated uranium and plutonium monopositive ions with 1,2,3,4,5-pentamethylcyclopentadiene (HCp*) are shown in Fig. 6. We tentatively assigned

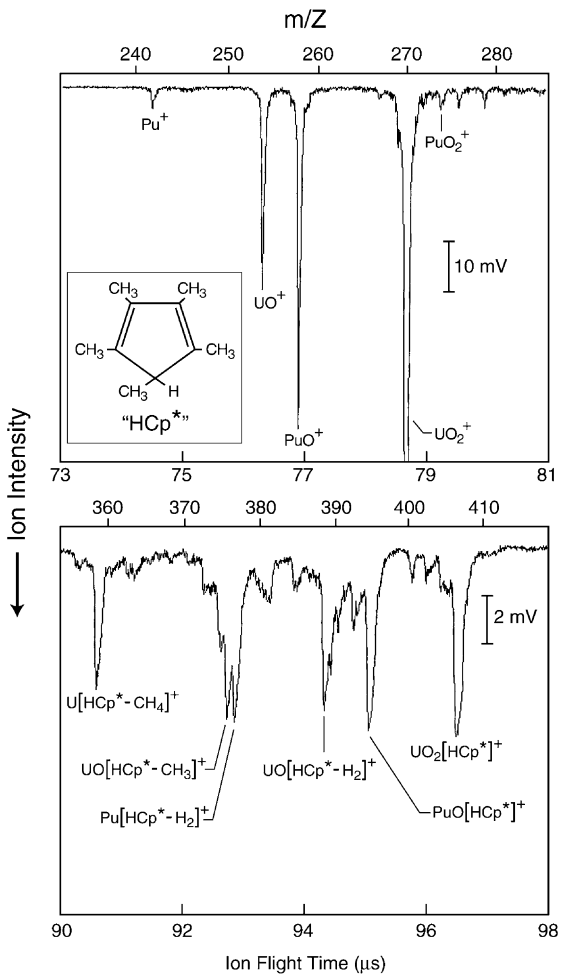

Fig. 6. LAPRD mass spectrum for the reaction of bare and oxo-ligated U and Pu monopositive ions with pentamethylcyclopentadiene. The panel trace shows the mass region of reactant ions and the lower panel shows the mass region with product ions.

all products as due to reaction with the moiety shown outside of brackets in the peak assignments. Thus, for example, $UO[HCp^*–H_2]^+$ was considered to result from H_2-loss from HCp^* induced by UO^+. In the case of uranium in particular, the large amount of ablated dioxide ion, UO_2^+, introduces the possibility of Reaction (2) [55]:

$$UO_2^+ + HCp^* \rightarrow UO[HCp^*–H_2]^+ + H_2O \qquad (2)$$

Because the OU^+–O bond dissociation energy is $740\,kJ\,mol^{-1}$, exothermic dehydration by Reaction (2) is thermodynamically improbable according to the same rationale already presented for dehydration by MO^+ with M^+–O bond energies of this magnitude. Nonetheless, it was desirable to definitively exclude this reaction to allow interpretation of the oxide reactivity results with a high degree of confidence. Accordingly, a series of experiments was carried out in a quadrupole ion trap mass spectrometer (QIT-MS) [56]. By performing mass-selective chemistry in the QIT-MS (experiments not possible by LAPRD), the reaction channels suggested by the product ion nomenclature employed in Fig. 6 were confirmed. In particular, Reaction (2) does not occur under near-thermal trapped ion conditions and UO^+-induced dehydrogenation of HCp^* is the pathway to $UO[HCp^*–H_2]^+$.

The results in Fig. 6 and for other An^+ reveal an unusually high reaction efficiency for the naked actinide ions with HCp^* [55]. The rather distinctive reactivity of HCp^* with An^+ is reminiscent of similar behavior previously reported for Ln^+ with this substrate [24,26]. It was established by QIT-MS that UO_2^+ is essentially inert, only forming addition products with HCp^*. The inert character of UO_2^+ is in accord with the FT-ICR studies with other reaction substrates, as already discussed. A particularly intriguing aspect of the results in Fig. 6 is the very different behaviors of UO^+ and PuO^+. The oxo-ligated uranium ion induced both CH_3-loss and H_2-loss whereas the corresponding plutonium monoxide ion was relatively inert under identical conditions, producing predominantly the adduct, $PuO[HCp^*]^+$. The reactivity of NpO^+ was also studied and behavior similar to that of PuO^+

was found. The initial interpretation of these results is that the 5f electrons at the metal center of UO^+ can participate in hydrocarbon activation by a direct insertion mechanism (Scheme 2), as suggested by Cornehl et al. [53]. The lower reactivities of NpO^+ and PuO^+ are consistent with increasing stabilization and localization of the 5f electrons as the nuclear charge increases. This hypothesis would predict diminishing reactivity in the order: $UO^+ > NpO^+ > PuO^+ > AmO^+ > CmO^+$. It was possible to study each of these oxides by LAPRD, except for AmO^+ which has a relatively small dissociation energy and was therefore ablated in insufficient quantities to allow detection of its reaction products. Both ThO^+ and UO^+ dehydrogenated cyclohexene with comparable efficiencies, much greater than that of CeO^+ [27], this in accord with the FT-ICR–MS results [53]. Subsequently, [42], it was found that UO^+ doubly-dehydrogenates cyclohexene while NpO^+ and PuO^+ are apparently inert. Also, UO^+ doubly-dehydrogenates cyclooctadiene while NpO^+ and PuO^+ both induce only single H_2-loss. These comparative reactivities are consistent with the HCp^* studies. Finally, the reactivity of CmO^+ [45] suggested a dehydrogenation activity of CmO^+ which is significantly less than that of UO^+ but greater than that of TbO^+. It could be inferred that the reactivity of CmO^+ is evidently somewhat greater than are the reactivities of NpO^+ and PuO^+. For example, whereas the latter two oxide ions were evidently inert towards 2-butene, CmO^+ dehydrogenated 1-butene.

The actinide oxide ion chemistry results obtained with LAPRD experiments are not as comprehensive as those for the bare actinide ions but are sufficient to conclude qualitatively that UO^+ is more reactive than the heavier AnO^+ but that the reactivity does not diminish significantly between NpO^+ and PuO^+, and evidently increases somewhat between PuO^+ and CmO^+ (AmO^+ was not studied). The proposition by Cornehl et al. [53] of participation of the 5f electrons of UO^+ at activation via an insertion mechanism could account for its enhanced reactivity. The absence of a significant decrease in reactivity beyond NpO^+ suggests a different activation mechanism for transuranic AnO^+ which does not involve direct insertion or participation of the 5f electrons (or empty 5f orbitals). A mechanism involving initial electrophilic interaction of lanthanide oxide cations with alkene π-systems was postulated to explain increasing reactivity with increasing electron affinity of the LnO^+, or, equivalently, increasing ionization energy (IE) of LnO [52]. For butadiene, onset of appreciable dehydrogenation/cracking occurred for IE[LnO] ∼ 6.2 eV (i.e., at HoO^+); for the more nucleophilic isoprene substrate, the reaction onset was lowered to IE[LnO] ∼ 5.6 eV (i.e., at TbO^+). For the actinide and lanthanide oxides studied in the present work, the ionization energies are [45,52,57] 6.1 eV for ThO; 5.7 eV for UO and NpO; 5.8 eV for PuO; >6.0 eV for CmO; 4.9 eV for CeO; and 5.6 eV for TbO. With the exceptions of ThO^+ (d-block behavior) and UO^+ (5f participation), the comparative reactivities are consistent with a mechanism initiated by electrophilic attack of MO^+ for both lanthanide and actinide oxide ions. In accord with this interpretation, a slightly greater reactivity of CmO^+ compared with NpO^+ and PuO^+ can be attributed to the greater electron affinity of CmO^+. A possible interpretation of the comparative monoxide ion reactivities—specifically the reduction in reactivity between UO^+ and NpO^+—is that a significant decrease in the involvement of the 5f electrons in bonding interactions during hydrocarbon activation occurs between UO^+ and NpO^+.

5. Reactions of actinide ions with other substrates

In addition to the emphasized reactions with hydrocarbons, gas-phase reactions of bare and oxo-ligated actinide ions have been carried out with several other types of substrates. In probably the earliest reported systematic study of gas-phase actinide ion chemistry, Moreland et al. [58] described endothermic reactions of U^+ and Pu^+ with hydrogen to produce UH^+ and PuH^+. An unexpected result of a recent LAPRD study was the evidently exothermic formation of "PuH_4^+" via reaction of Pu^+ with ethylene oxide; analogous

results were found for other actinide ions [59]. Further recent examination of this phenomenon has suggested that these "tetrahydride" peaks were actually a result of an unusual experimental phenomenon and not to a metal ion–molecule reaction as previously proposed; these anomalous results will be described in detail elsewhere.

The simple oxidation of U^+ by O_2 has been studied in some detail. Johnson and Biondi [60] first showed that the O-abstraction reaction, $U^+ + O_2 \rightarrow UO^+ + O$, is exothermic (in contrast, N-abstraction from N_2 was found to be endothermic). Subsequently, it was shown by Armentrout and Beauchamp [54] that this oxidation reaction proceeds with essentially no activation barrier. The oxidation of actinide and actinide oxide ions by ethylene oxide was studied by LAPRD [59]. The exothermic oxidation of PuO^+ to $PuO_2{}^+$ indicates that the OPu^+–O bond energy is at least 350 kJ mol^{-1}, which is substantially greater than previous estimates. A particularly interesting example of oxidation of uranium ions was the exothermic formation of the stable free doubly-charged uranyl ion, $UO_2{}^{2+}$, via sequential abstraction of two O-atoms from dioxygen by U^{2+} [61]. Heinemann and Schwarz also produced the molecular ion NUO^+, which is isoelectronic with $UO_2{}^{2+}$, by the reaction of U^+ with N_2O to generate UN^+ for subsequent reaction with O_2 to give NUO^+ [62].

The guided ion beam apparatus in the laboratory of Beauchamp was also employed to study reactions of U^+ with N_2, D_2 (and CD_4, as already discussed) [36], CO, CO_2, COS, CS_2, D_2O [54], CH_3F, SiF_4, CH_3Cl and CCl_4 [63]. The reaction with CH_3F exothermically produced UF^+ and that with $SiF_4{}^+$ endothermically produced $UF_2{}^+$. Under the approximately thermoneutral reaction conditions of LAPRD, reactions of actinide ions with perfluorophenanthrene ($C_{14}F_{24}$) and other fluorocarbons were found to result in $AnF_n{}^+$, presumably by F-abstraction rather than a mechanism involving An^+-insertion, with the highest observed value of "*n*" reflecting the relative stabilities of the higher actinide oxidation states [64]. For example, $NpF_3{}^+$ was formed when $AnF_2{}^+$ were the terminal products for An=Pu and Am; the highest fluoride observed was $UF_4{}^+$. As an indication of the stability of uranium in high oxidation states, UF^{3+} has been experimentally observed and is predicted to be stable towards Coulomb explosion, a manifestation of the unusually low third ionization energy of uranium [65].

Motivations for investigating gas-phase reactions of metal ions with functionalized hydrocarbons have been discussed by Eller [66]. A primary interest is the effect of the functional group on the initial interaction with the metal ion, and the resulting mechanisms and reaction pathways. Reactions of actinide ions with nitriles and butylamine were studied by LAPRD for comparison with the hydrocarbon results to probe effects of the nitrogen functionality on interactions of actinide ions with organic substrates [67]. Nitriles, with their electron rich C≡N: moiety, were found to be rather effective complexing agents for both An^+ and AnO^+. Additionally, dehydrogenation proceeded for Th^+, U^+ and Np^+ which is attributed to the ability for their facile insertion into C–H bonds. Similarly, butylamine was dehydrogenated by Np^+ but formed primarily adducts with Am^+. In contrast, both NpO^+ and AmO^+ rather efficiently dehydrogenated butylamine, presumably via a multi-centered electrostatically bonded intermediate (similar to Scheme 3).

Reactions of f-element ions with oxygen-containing organic molecules offers the opportunity to activate C–O and O–H bonds with formation of products which incorporate metal–oxygen bonds. The formation of such products is expected to be particularly important for the oxophilic lanthanides and actinides. Lanthanide ions, Ln^+, were shown by FT-ICR–MS to efficiently react with phenol to give $LnOH^+$ and/or LnO^+, with the notable exception of Yb^+ [68]. Similar studies with trimethylformate, $HC(OCH_3)_3$, resulted in mono- and bis-lanthanide methoxide ions, $Ln(OCH_3)_{1,2}{}^+$ [69]. We have studied reactions of An^+ with alcohols and dimethyl ether [70]. With alcohols, both hydroxides (C–O activation) and alkoxides (O–H activation) were produced with stoichiometries in accord with the propensities of the actinides to exist in particular oxidation states; for example, simultaneous reaction of Np^+ and Am^+ with propanol resulted in a substantially greater yield of

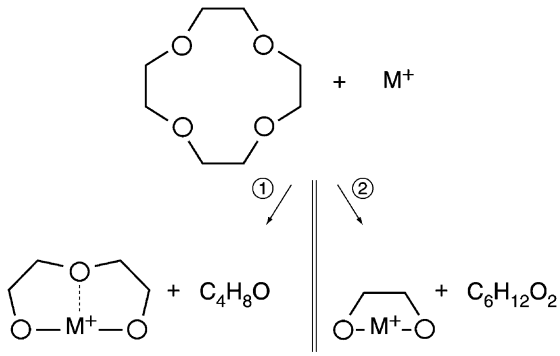

Scheme 4.

the bis-propoxide, $An(OC_3H_7)_2^+$, for Np. Similarly, simultaneous reaction with dimethylether produced primarily $Am(OCH_3^+)$ and $Np(OCH_3)_2^+$.

Recently, we have extended our studies of actinide ion–ether reactions to cyclic ethers, including 12-crown-4 ether (shown at the top of Scheme 4) [71]. Whereas 12-crown-4 ether was shown to associate with metal ions such as K^+, reaction with An^+ resulted in a variety of complex product ions, such as those identified for plutonium in the LAPRD mass spectrum in Fig. 7; postulated metallaoxocycle products are shown in Scheme 4 where M = Pu. Although naked actinide ions such as Pu^+ destroy the crown ether structure and bonding in the gas phase, the $Pu(OH)_2C_8H_{16}O_4^+$ association complex peak evident in Fig. 7 demonstrates the possibility to explore relative association efficiencies of ligated actinide ions. Complexation of crown ethers with metal ions has been an active area of gas-phase metal ion chemistry for several years and studies with actinides are relevant to better understanding the solution phase chemistry of these elements.

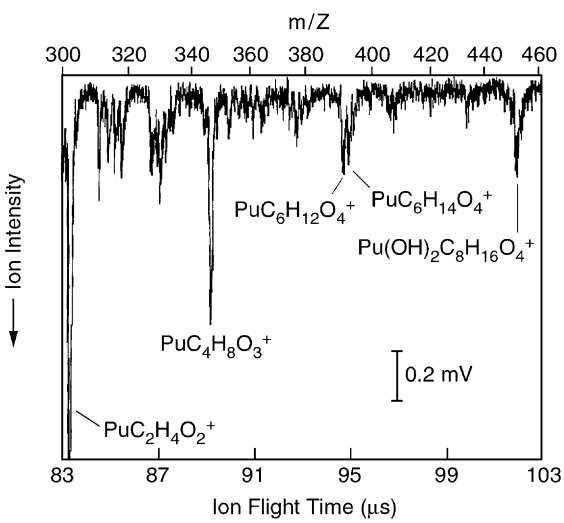

Fig. 7. Portion of the LAPRD product mass spectrum for the reaction of Pu^+ with 12-crown-4 ether.

Recently, da Conceição Vieira et al. [72] reported on reactions of Th^+ and U^+ (and Ln^+) with $Fe(CO)_5$ and $Fe(C_5H_5)_2$. Reactions with the carbonyl resulted in $MFe(CO)_x^+$ with evidence for direct M–Fe bonding. Reactions with the bis-cyclopentadienyl complex resulted in the $An(C_5H_5)_2^+$ complexes. With some lanthanides, adducts such as $SmFe(C_5H_5)_2^+$ were also observed in this study; $AnFe(C_5H_5)_2^+$ were likely intermediates in the An/Fe exchange reactions.

6. Future prospects in gas-phase actinide ion chemistry

The results already summarized demonstrate the value of gas-phase actinide ion chemistry as a route to a better understanding of the unique electronic structures, energetics and bonding behavior of these elements. Due to the difficulties associated with performing conventional chemistry with most of the actinide elements, gas-phase ion techniques are particularly appealing in this region of the periodic table. In particular, such studies promise to illuminate the nature of the 5f electrons, as well as relativistic effects which underlie much of the physicochemical behavior of heavy elements, primarily as a result of the increased stabilization of orbitals with high electron density in the vicinity of the highly-charged nucleus. In essence, these types of studies enhance our fundamental understanding of the periodic chemical behavior of the elements. To date rather little theoretical effort has been directed

towards understanding and predicting gas-phase actinide ion chemistry. In view of the obstacles to experimental studies of these elements it would be particularly valuable to employ the expanding base of experimental results to further develop theoretical models to understand and predict the chemistry of actinides.

Trapped ion mass spectrometry studies will continue to be extended to the more highly radioactive actinides, as they have previously been to thorium and uranium. Both FT-ICR–MS and QIT-MS techniques are applicable and have the capability for versatile ion selection and manipulation. These techniques operate in different regimes of pressure and other experimental parameters and are complementary approaches. The Paul trap is generally more compact than the Penning trap and is accordingly better-suited for incorporation into alpha-containment gloveboxes for the study of the most highly radioactive actinides. A priority will be on obtaining absolute reaction rates with a variety of reactant molecules for quantitative assessment of relative actinide ion reactivities. One goal is to detect reactivity differences among the light actinides which may be attributable to participation of the 5f electrons. The heavier actinides are unlikely to exhibit direct participation of the 5f electrons but quantification of their reactivities can serve to more fully evaluate the accuracy and relevance of the spectroscopically determined electronic structures and energetics. Whereas the LAPRD approach was unable to effectively differentiate between relatively unreactive actinide ions such as Am^+ and Cf^+, trapped ion techniques should provide enhanced resolution in such cases. For Cf^+ and Fm^+, the reported excitation energies are only estimates and it should be possible to assess the accuracy of these values. Guided ion beam studies of transuranic actinides would be of great value for the quantitative assessments of actinide ion reaction thermochemistry. However, as with the trapping techniques, radioactive contamination is a major obstacle to ion beam studies of reaction pathways as a function of collisional energy.

There are several other attributes of trapped ion mass spectrometry studies which will shed light on fundamental actinide chemistry. Studies of reactions with a variety of reagents under nearly thermoneutral conditions can be employed to "bracket" thermochemical quantities such as bond dissociation energies. Collision induced dissociation might provide structural and qualitative thermochemical information for selected (simple) systems. The kinetic method might also be applied to assessing bond strengths in organoactinide complexes. Mass-selective chemistry will enable the systematic study of the effects of ligation and complexation on the electronic structure and chemical activity of the metal center. The discussed effects of oxo-ligation are but one example of such effects. It will be possible to study multiply charged ions; previous results for Th^{2+} and U^{2+} suggested chemically active 5f electrons but it is necessary to extend these studies to transuranic actinides to effectively interpret these results. In this regard, it is noted that very recently the first studies of gas-phase transuranium ion chemistry by FT-ICR–MS were carried out with Np-237 and Pu-242 [73].

Whether by trapped ion techniques or by a transient technique such as LAPRD, the chemistry of bare and ligated protactinium ions should be further pursued because this is the region of the actinide series where involvement of the 5f electrons should be maximized. It is also desirable to study the chemistries of Ac^+ and AcO^+. The bare actinium ion has a ground state configuration of $[Rn]7s^2$ with no 5f electrons and a promotion energy of 0.6 eV to the $[Rn]6d^17s^1$ chemically active configuration: Ac^+ provides an opportunity to further assess the inert nature of the closed-shell $7s^2$ configuration and a basis to assess the effects of introduction of 5f electrons upon proceeding beyond Ac to the 5f members of the actinide series. The dissociation energy of AcO^+ (and AcO) is unknown but is predicted to be similar to that of LaO^+, ~9 eV. It would be of value to both determine the actual dissociation energy (e.g., by CID) and to study the chemistry of AcO^+ because it has no valence electrons at the metal center and thus provides a basis to assess the behavior of the heavier AnO^+.

The study of the chemistry of the elements beyond Fm can effectively be carried out using only one

atom at a time because of the very low production rates and short half-lives of the available nuclides of these elements [74]. Elementary aspects of the gas-phase chemistry of neutral heavy actinides and transactinides through bohrium (element 107) have been determined employing elegant nuclear counting techniques in conjunction with calibration using radioactive isotopes of elements for which the chemistry is well known [75]. The prospect of gas-phase ion chemistry of heavy (transfermium) actinide and transactinide elements is an appealing approach to elucidating this region of the periodic table. Key issues to be addressed in greater detail include the increasing importance of relativistic effects with increasing nuclear charge [76]. The information which can be gleaned from reactions of metal ions with hydrocarbons would be invaluable in directly addressing central questions regarding the structure of the periodic table. One question which might feasibly be addressed is whether the ground state configuration of Lr^+ is $[Rn]5f^{14}7s^2$, and if relativistic stabilization of the $[Rn]5f^{14}7s^17p^1_{1/2}$ configuration results in a sufficiently small excitation energy that enhanced chemical reactivity of Lr^+ is exhibited. Although such experiments would be extremely challenging, several elements of interest should be available on-line in sufficient quantities and with adequately long half-lives to allow ingenious investigations. A sophisticated ion trap facility, "SHIPTRAP," is being developed at GSI Darmstadt for the capture and storage of heavy radionuclides [77]. Among the proposed applications of this unique accelerator-based ion trap is the study of the chemistry of transeinsteinium elements.

The synthesis and chemistry of actinide clusters ions is another promising avenue of pursuit. These nanostructures offer a link between the molecular and solid states of matter, and can exhibit characteristics not exhibited by either. Clusters may also enhance our understanding of interfacial chemistry of technologically important actinides such as Pu. We have successfully synthesized and demonstrated the ability to study chemistry of plutonium oxide clusters of various sizes and plutonium oxidation states [78]. An important issue which could be addressed by studying plutonium oxide cluster ion chemistry is the water-catalyzed oxidation of plutonium dioxide to a hyperstoichiometric oxide, PuO_{2+x}. This unexpected phenomenon is of great importance in understanding and predicting the behavior of plutonium in storage and environmental conditions [79,80]. The ability to mass-select clusters of specific size and oxidation state makes trapped ion techniques particularly attractive for this general avenue of inquiry.

Acknowledgements

This work was sponsored by the Division of Chemical Sciences, Geosciences and Biosciences, U.S. Department of Energy, under Contract DE-AC05-00OR22725 with Oak Ridge National Laboratory, managed and operated by UT-Battelle, LLC. The author is grateful to Dr. J. Marçalo and the reviewers for helpful comments.

References

[1] S.K. Searles, P. Kebarle, Can. J. Chem. 47 (1969) 2619–2626.
[2] I. Dzidic, P. Kebarle, J. Phys. Chem. 74 (1970) 1466–1474.
[3] R.H. Staley, J.L. Beauchamp, J. Am. Chem. Soc. 97 (1975) 5920–5921.
[4] J. Allison, D.P. Ridge, J. Am. Chem. Soc. 99 (1977) 35–39.
[5] J. Allison, R.B. Freas, D.P. Ridge, J. Am. Chem. Soc. 101 (1979) 1332–1333.
[6] P.B. Armentrout, in: D.H. Russell (Ed.), Gas Phase Inorganic Chemistry, Plenum Press, New York, 1989, pp. 1–42.
[7] K. Eller, H. Schwarz, Chem. Rev. 91 (1991) 1121–1177.
[8] J.C. Weisshaar, Acc. Chem. Res. 26 (1993) 213–219.
[9] B.S. Freiser, Acc. Chem. Res. 27 (1994) 353–360.
[10] K. Seemeyer, D. Schröder, M. Kempf, O. Lettau, J. Müller, H. Schwarz, Organometallics 14 (1995) 4465–4470.
[11] B.S. Freiser, J. Mass Spectrom. 31 (1996) 703–715.
[12] P.A.M. Van Koppen, P.R. Kemper, M.T. Bowers, in: B.S. Freiser (Ed.), Organometallic Ion Chemistry, Kluwer, Dordrecht, 1996, pp. 157–196.
[13] K.J. Fisher, I.G. Dance, G.D. Willett, Rapid Commun. Mass Spectrom. 10 (1996) 106–109.
[14] G.T. Seaborg, Radiochim. Acta 61 (1993) 115–122.
[15] J.L. Thomas, R.G. Hayes, J. Organometall. Chem. 23 (1970) 487–489.
[16] Y. Huang, M.B. Wise, D.B. Jacobson, B.S. Freiser, Organometallics 6 (1987) 346–354.

[17] J.B. Schilling, J.L. Beauchamp, J. Am. Chem. Soc. 110 (1988) 15–24.
[18] L.S. Sunderlin, P.B. Armentrout, J. Am. Chem. Soc. 111 (1989) 3845–3855.
[19] Y.A. Ranasinghe, T.J. MacMahon, B.S. Freiser, J. Am. Chem. Soc. 114 (1992) 9112–9118.
[20] Y.A. Ranasinghe, B.S. Freiser, Chem. Phys. Lett. 200 (1992) 135–141.
[21] W.W. Yin, A.G. Marshall, J. Marçalo, A. Pires de Matos, J. Am. Chem. Soc. 116 (1994) 8666–8672.
[22] C. Heinemann, D. Schröder, H. Schwarz, Chem. Ber. 127 (1994) 1807–1810.
[23] H.H. Cornehl, C. Heinemann, D. Schröder, H. Schwarz, Organometallics 14 (1995) 992–999.
[24] J. Marçalo, A. Pires de Matos, W.J. Evans, Organometallics 15 (1996) 345–349.
[25] J.K. Gibson, J. Phys. Chem. 100 (1996) 15688–15694.
[26] J. Marçalo, A. Pires de Matos, W.J. Evans, Organometallics 16 (1997) 3845–3850.
[27] J.K. Gibson, Organometallics 16 (1997) 4214–4222.
[28] M.A. Tolbert, J.L. Beauchamp, J. Am. Chem. Soc. 106 (1984) 8117–8122.
[29] F.A. Cotton, G. Wilkinson, Advanced Inorganic Chemistry, 5th Edition, Wiley, New York, 1988, pp. 955–1017.
[30] W.C. Martin, R. Zalubas, L. Hagan, Atomic Energy Levels—The Rare-Earth Elements, NBS (NIST), Washington, DC, 1978.
[31] J.J. Katz, L.R. Morss, G.T. Seaborg, in: J.J. Katz, G.T. Seaborg, L.R. Morss (Eds.), The Chemistry of the Actinide Elements, 2nd Edition, Chapman & Hall, London, 1986, pp. 1121–1195.
[32] M.V. Nevitt, M.B. Brodsky, in: J.J. Katz, G.T. Seaborg, L.R. Morss (Eds.), The Chemistry of the Actinide Elements, 2nd Edition, Chapman & Hall, London, 1986, pp. 1388–1416.
[33] J. Blaise, J.-F. Wyart, International Tables of Selected Constants, Energy Levels and Atomic Spectra of Actinides, Vol. 20, Tables of Constants and Numerical Data (Tables de Constantes et Données Numériques), Paris, 1992.
[34] L. Brewer, J. Opt. Soc. Am. 61 (1971) 1666–1682.
[35] D. Schröder, S. Shaik, H. Schwarz, Acc. Chem. Res. 33 (2000) 139–145.
[36] P. Armentrout, R. Hodges, J.L. Beauchamp, J. Am. Chem. Soc. 99 (1977) 3162–3163.
[37] P.B. Armentrout, R.V. Hodges, J.L. Beauchamp, J. Chem. Phys. 66 (1977) 4683–4688.
[38] Z. Liang, A.G. Marshall, A. Pires de Matos, J.C. Spirlet, in: L.R. Morss, J. Fuger (Eds.), Transuranium Elements: A Half Century, American Chemical Society, Washington, DC, 1992, pp. 247–250.
[39] C. Heinemann, H.H. Cornehl, H. Schwarz, J. Organometall. Chem. 501 (1995) 201–209.
[40] J. Marçalo, J.P. Leal, A. Pires de Matos, Int. J. Mass Spectrom. Ion Processes 157/158 (1996) 265–274.
[41] J. Marçalo, J.P. Leal, A. Pires de Matos, A.G. Marshall, Organometallics 16 (1997) 4581–4588.
[42] J.K. Gibson, J. Am. Chem. Soc. 120 (1998) 2633–2640.
[43] H. Higashide, T. Oka, K. Kasatani, H. Shinohara, H. Sato, Chem. Phys. Lett. 163 (1989) 485–489.
[44] J.K. Gibson, Organometallics 17 (1998) 2583–2589.
[45] J.K. Gibson, R.G. Haire, J. Phys. Chem. A 102 (1998) 10746–10753.
[46] J.K. Gibson, R.G. Haire, Radiochim. Acta, in press.
[47] J.K. Gibson, R.G. Haire, Int. J. Mass Spectrom. 203 (2000) 127–142.
[48] J.K. Gibson, R.G. Haire, unpublished results.
[49] J.K. Gibson, R.G. Haire, unpublished results.
[50] D. Schröder, H. Schwarz, Angew. Chem. Int. Ed. Engl. 34 (1995) 1973–1995.
[51] D. Schröder, H. Schwarz, S. Shaik, in: B. Meunier (Ed.), Metal-Oxo and Metal-Peroxo Species in Catalytic Oxidations, Springer, Berlin, 2000, pp. 91–123.
[52] H.H. Cornehl, R. Wesendrup, J.N. Harvey, H. Schwarz, J. Chem. Soc., Perkin Trans. 2 (1997) 2283–2291.
[53] H.H. Cornehl, R. Wesendrup, M. Diefenbach, H. Schwarz, Chem. Eur. J. 3 (1997) 1083–1090.
[54] P.B. Armentrout, J.L. Beauchamp, Chem. Phys. 50 (1980) 21–25.
[55] J.K. Gibson, Int. J. Mass Spectrom. 202 (2000) 19–29.
[56] D.C. Duckworth, J.K. Gibson, in: Proceedings of the 48th ASMS Conference on Mass Spectrometry and Allied Topics, American Society of Mass Spectrometry, Santa Fe, NM, 2000, pp. 225–226.
[57] D.L. Hildenbrand, L.V. Gurvich, V.S. Yungman, The Chemical Thermodynamics of Actinide Elements and Compounds, Part 13, The Gaseous Actinide Ions, IAEA, Vienna, 1985.
[58] P.E. Moreland, D.J. Rokop, C.M. Stevens, Int. J. Mass Spectrom. Ion Phys. 5 (1970) 127–136.
[59] J.K. Gibson, J. Mass Spectrom. 36 (2001) 284–293.
[60] R. Johnson, M.A. Biondi, J. Chem. Phys. 57 (1972) 1975–1979.
[61] H.H. Cornehl, C. Heinemann, J. Marçalo, A. Pires de Matos, H. Schwarz, Angew. Chem. Int. Ed. Engl. 35 (1996) 891–894.
[62] C. Heinemann, H. Schwarz, Chem. Eur. J. 1 (1995) 7–11.
[63] P.B. Armentrout, J.L. Beauchamp, J. Phys. Chem. 85 (1981) 4103–4105.
[64] J.K. Gibson, Radiochim. Acta 84 (1999) 135–146.
[65] D. Schröder, M. Diefenbach, T.M. Klapotke, H. Schwarz, Angew. Chem. Int. Ed. Engl. 38 (1999) 137–140.
[66] K. Eller, in: B.S. Freiser (Ed.), Organometallic Ion Chemistry, Kluwer, Dordrecht, 1996, pp. 123–155.
[67] J.K. Gibson, Inorg. Chem. 38 (1999) 165–173.
[68] J.M. Carretas, A. Pires de Matos, J. Marçalo, M. Pissavini, M. Decouzon, S. Geribaldi, J. Am. Soc. Mass Spectrom. 9 (1998) 1035–1042.
[69] N. Marchandé, S. Breton, S. Géribaldi, J.M. Carretas, A. Pires de Matos, J. Marçalo, Int. J. Mass Spectrom. 195/196 (2000) 139–148.
[70] J.K. Gibson, J. Mass Spectrom. 34 (1999) 1166–1177.
[71] J.K. Gibson, unpublished results.
[72] M. da Conceição Vieira, J. Marçalo, A. Pires de Matos, J. Organometall. Chem. 632 (2001) 1166–1177.

[73] M. Santos, J. Marçalo, A. Pires de Matos, J.K. Gibson, R.G. Haire, unpublished results.
[74] D.C. Hoffman, Radiochim. Acta 61 (1993) 123–128.
[75] R. Eichler, et al., Nature 407 (2000) 63–65.
[76] O.L. Keller Jr., Radiochim. Acta 37 (1984) 169–180.
[77] J. Dilling, et al., Hyperfine Interact. 127 (2000) 491–496.
[78] J.K. Gibson, R.G. Haire, J. Alloys Compounds 322 (2001) 143–152.
[79] J.M. Hashke, T.H. Allen, L.A. Morales, Science 287 (2000) 285–287.
[80] C. Madic, Science 287 (2000) 243–244.